PARAMAGNETIC COOLING

PARAMAGNETIC COOLING

BY

ROBERT HONG HUM, B.Sc.

A Thesis

Submitted to the Faculty of Graduate Studies

in Partial Fulfilment of the Requirements

for the Degree

Master of Science

McMaster University

October 1965

MASTER OF SCIENCE (1965)
(Physics)

McMASTER UNIVERSITY
Hamilton, Ontario.

TITLE: Paramagnetic Cooling

AUTHOR: Robert Hong Hum, B.Sc. (Carleton University)

SUPERVISOR: Professor C. K. Campbell

NUMBER OF PAGES: vi, 48

SCOPE AND CONTENTS:

A metal adiabatic demagnetization cryostat was designed and constructed. The final-temperature dependence of a single-crystal synthetic ruby was investigated as a function of applied magnetic field. The ruby was used both as a thermometer and coolant in superconducting thin-film experiments at temperatures below 1°K. Difficulties encountered in these experiments have been discussed in detail. Further improvements on the system have been suggested in the application of thin-film superconductor studies.

ABSTRACT

We have constructed an adiabatic demagnetization cryostat with a non-ferromagnetic stainless steel chamber. A single-crystal synthetic ruby was used as the paramagnetic salt. The final-temperature dependence on the applied magnetic field, generated by a superconducting magnet, was investigated. The results obtained agree fairly well with an extremely simple theoretical calculation within the limits of the theory. Temperatures below 1°K were measured by a susceptibility thermometer using the a-c method.

Superconductive tunnel junctions were evaporated onto the flat end of the ruby crystal and attempts were made to observe the properties of these junctions at low temperatures using the ruby as a coolant. Difficulties involved and suggestions on improvements for future thin-film experiments have been discussed.

ACKNOWLEDGEMENT

The author wishes to express his sincerest thanks to Dr. C. K. Campbell for his constant guidance, interest and encouragement throughout the work of this thesis.

This research was supported by the grants-in-aid to Dr. C. K. Campbell from the National Research Council of Canada. The author is also indebted to the Province of Ontario for the Province of Ontario Graduate Fellowship award.

TABLE OF CONTENTS

CHAPTER I

INTRODUCTION

1.1 LOW TEMPERATURE PHYSICS

For the past half century, the field of low temperature research has revealed many new problems and phenomena. The first successful step in this field was the liquefaction of the permanent gases. Ultimately, helium was liquefied at the temperature of 4.2°K at atmospheric pressure.

One of the pioneers of this field was Nernest, whose work eventually led to the Third Law of Thermodynamics. The object of Nernest's work was to find a reference point for the calculation of chemical equilibria. Obviously, absolute zero was clearly the most suitable condition in which different substances might be compared with each other. It is believed that all kinetic motion ends and the state of complete rest is achieved at absolute zero. Nernest also concluded that it is not the energy but the entropy that vanishes at T=0°K. With this new concept, problems of specific heat and zero point free energy took a new stand. After the introduction of quantum theory, many more physical phenomena were explained. Phenomenon such as the specific heat of solids at low temperatures was made clear by quantization of the lattice vibrations. Low temperature

research not only plays a large part in the investigation of the existing problems in solid state physics but it has also brought up some new and strange phenomena such as superconductivity and superfluidity which seem to be completely divorced from any other manifestation of the laws of physics.

1.2 RECENT AND PAST DEVELOPMENTS OF LOW TEMPERATURE SOURCES

The Third Law of Thermodynamics (1) states that it is impossible by any procedure no matter how idealized to reduce any system to the absolute zero of temperature in a finite number of operations. In spite of this statement, scientists all over the world have tried by one means or another to reduce the temperature as close to absolute zero as possible. Following the liquefaction of helium at atmospheric pressure, temperatures in the order of $1^{\circ}K$ were obtained fairly easily by reducing the surface vapour pressure of the liquid through mechanical pumping, thereby removing some of the more energetic molecules from the system. It is to be noted however, that the physical requirements on the pump size place this lower limit on the temperatures that can be achieved by this method.

As early as the 1920's, the means of attaining temperatures below $1^{\circ}K$ were discovered. The first proposal for a new method was published in 1926, independently by Debye (2) and Giauque (3). In 1933, the experimental results of this method were reported simultaneously from Berkeley (4), Leiden (5) and Oxford (6). This method is now known as the process of adiabatic demagnetization

or magnetic cooling. With this method, temperature attainments in the order of millidegrees were reported as applied to certain paramagnetic salts.

Other methods of obtaining low temperatures include adiabatic magnetization of superconductors (7), mechanocaloric effect in liquid helium II (8), and more recently developed ones such as He^3 and nuclear demagnetization (9) which give temperatures as low as $0.3^{o}K$ and $2x10^{-5}\ ^{o}K$ respectively.

1.3 PROBLEMS AND APPLICATIONS OF LOW TEMPERATURE SOURCES

In all of the above mentioned methods of obtaining low temperatures it may be appreciated that the number of substances which can be used as a cooling agent is limited. This is especially true if the substance is to be used to cool another normally unsuitable material which requires investigation at such reduced temperatures. Problems of thermal contact and isolation are introduced which further complicate the measurement and interpretation of temperature observations on systems below $1^{o}K$.

1.4 AIMS OF THIS THESIS

In this thesis, we are interested in attaining temperatures of about $0.3^{o}K$ with reasonable ease and with economy and simplicity in the construction of apparatus. To this end we have chosen the method of magnetic cooling, using a paramagnetic salt energized by a superconducting magnet. A ruby crystal was chosen as the active paramagnetic salt for these demagnetization experiments. Such a crystal, initially employed in a laser system, was readily

available for experimentation. This choice was made for the following reasons. Experiments by other observers had been reported on the paramagnetic properties of such a material when used as a thermometer below 1°K (10). In view of this, it was felt that its investigation as an active demagnetization coolant would be profitable, especially after consideration of the high thermal conductivity characteristics of ruby at low temperatures. The aim of the thesis, therefore, was to study the temperature-magnetic field characteristics of such a substance when used as the active coolant in a demagnetization cryostat. Another aim, inspired by the geometry of the available crystal, was the possible study of tunneling phenomena in thin-film superconductor fabrications which might readily be attached to the crystal.

CHAPTER II

THEORY OF PARAMAGNETIC COOLING

2.1 PARAMAGNETISM

Substances with a positive susceptibility are called paramagnetics. The magnetic susceptibility per unit volume is defined as:

$$\chi = \frac{M}{H}, \tag{2.1}$$

where M is the magnetic moment per unit volume or the magnetization and H is the magnetic field intensity.

Electronic paramagnetism is found in:

(i) many atoms and molecules possessing an odd number of electrons since the total spin of such a system can not be zero.

(ii) many free atoms and ions with a partly filled inner shell.

(iii) metals in which paramagnetism arises from conduction electrons.

2.1a THE LANGEVIN-DEBYE THEORY OF PARAMAGNETISM

The atomic theory of paramagnetism connecting the magnetization with the permanent magnetic moments of the molecules or ions was first developed by Langevin on the

basis of classical theory. This theory was extended by Debye into a quantum mechanical or theoretical form.

In classical theory, the interaction between the magnetic dipoles is assumed to be weak and these dipoles also assumed to be freely rotating so that the field in which a given dipole finds itself is equal to the applied field $\bar{H}$. The resulting magnetic moment $\bar{M}$ per unit volume is then given as

$$M = N\mu L\left(\frac{\mu H}{kT}\right), \tag{2.2}$$

where k is Boltzmann's constant, T is the temperature in degrees Kelvin, N is the number of magnetic dipole moments, $\bar{\mu}$, per unit volume and $L\left(\frac{\mu H}{kT}\right)$ is the Langevin function which is

$$L\left(\frac{\mu H}{kT}\right) = \coth\left(\frac{\mu H}{kT}\right) - \frac{\mu H}{kT}. \tag{2.3}$$

If $\mu H \ll kT$, equation (2.2) reduces to

$$M \simeq \frac{N\mu^2 H}{3kT}, \tag{2.4}$$

or

$$\chi = \frac{M}{H} \simeq \frac{N\mu^2}{3kT}. \tag{2.5}$$

μ here is of the order of one Bohr magneton, so at room temperature and a field of 10^4 gauss we have

$$\frac{\mu H}{kT} \approx \frac{1}{400.} \qquad (2.6)$$

Thus, for normally available magnetic fields, the above condition is satisfied except at very low temperatures. We note that equation (2.5) indicates that

$$\chi = \frac{C}{T}, \qquad (2.7)$$

where C is a constant known as the Curie Constant. Equation (2.7) is known as the Curie Law.

In quantum theory, the permanent magnetic dipoles of a given atom or ion is not freely rotating but are restricted to a finite set of orientations relative to the applied field. The possible components of the magnetic moment are

$$M_J g \mu_B, \text{ where } M_J = J, (J-1), \ldots\ldots, -(J-1), -J.$$

J here is the total angular momentum quantum number, μ_B is the Bohr magneton and g is the Lande g factor or the spectroscopic splitting factor which is given as

$$g = \frac{3J(J+1)+S(S+1)-L(L+1)}{2J(J+1)} \qquad (2.8)$$

where S and L are spin and orbital quantum members respectively.

The potential energy V of a dipole of moment $\bar{\mu}$ in a field $\bar{H}$ is

$$V = -\bar{\mu}\cdot\bar{H}. \qquad (2.9)$$

Thus, the potential energy of a magnetic dipole with a component $M_J g\mu_B$ along H is $-M_J g\mu_B H$. According to Boltzmann statistics the total magnetization is

$$M = \frac{N\sum_{-J}^{+J} M_J g\mu_B \exp\left(M_J g\mu_B H/kT\right)}{\sum_{-J}^{+J} \exp\left(M_J g\mu_B H/kT\right)}. \qquad (2.10)$$

In order to obtain a simpler expression for equation (2.10), we may consider two cases.

Case 1: $M_J g\mu_B H << kT$. In this case (2.10) reduces to

$$M = \frac{Ng^2 J(J+1)\mu_B^2 H}{3kT},$$

$$\text{or} \quad \chi \equiv \frac{M}{H} = \frac{Ng^2 J(J+1)\mu_B^2}{3kT}. \qquad (2.11)$$

This is identical to equation (2.5) except that the total magnetic moment μ_J associated with J is now given by

$$\mu_J^2 = g^2 J(J+1)\mu_B^2. \qquad (2.12)$$

Hence, the Curie Law holds in this range of temperatures even in quantum theory.

Case 2: At low temperatures where $N_J g\mu_B H$ is comparable to kT, we can not use the approximation as in Case 1. Equation (2.10) then reduces to

$$M = NgJ\mu_B B_J(Jg\mu_B H/kT), \tag{2.13}$$

where $B_J(Jg\mu_B H/kT)$ is called the Brillouin function and is defined by

$$B_J\left(Jg\mu_B H/kT\right) = \frac{2J+1}{2J}\coth\left[\frac{2J+1}{2J}\left(\frac{Jg\mu_B H}{kT}\right)\right] - \frac{1}{2J}\coth\left[\frac{1}{2J}\left(\frac{Jg\mu_B H}{kT}\right)\right]. \tag{2.14}$$

On extending this theory, Weiss took into consideration the interaction between the magnetic dipoles and assumed that the total field experienced by these dipoles when an external magnetic field is applied must include a term which is proportional to the magnetization of the substance, that is,

$$H_m = H_a + DM, \tag{2.15}$$

where H_m is the Weiss molecular field (total field), H_a is the applied field and D is the Weiss field constant which depends on the geometry of the substance. Now if we consider the susceptibility just above the Curie temperature below which the material becomes a ferromagnet and postulate that the Curie Law holds, the total field is the sum of the applied field and the field due to

the magnetization. Hence,

$$\frac{M}{H_a + DM} = \frac{C}{T}. \tag{2.16}$$

Thus $$\chi = \frac{M}{H_a} = \frac{C}{T - CD}. \tag{2.17}$$

This gives a non-zero magnetization for zero applied field at the Curie point given by

$$\Delta = CD, \tag{2.18}$$

and $\chi = \frac{C}{T-\Delta}$ is known as the Curie-Weiss Law.

2.2 PARAMAGNETIC COOLING

2.2a THERMODYNAMICS

A low temperature thermodynamic system is characterized not only by low energy but also by low entropy. For any refrigeration process, a working substance is needed whose entropy depends both on the temperature and on an external variable parameter. Thus the entropy of the working substance can be decreased by varying the parameter isothermally. This means that the temperature dependent part of the entropy remains constant. Suppose the decrease in entropy, due to the variation of the parameter, is ΔS, then the amount of heat ΔQ removed from the substance is

$$\Delta Q = T\Delta S, \tag{2.19}$$

where T is the temperature of the substance during the variation. Now, if the parameter is varied in the opposite direction adiabatically, the entropy of the whole system, i.e., the working substance, remains constant. In order for the system to achieve thermal equilibrium, part of the entropy due to the temperature-dependence must be given to that of the parameter part. This shift of entropy will be accompanied by a fall in temperature of the whole system.

The concept of the above may be illustrated clearly with the aid of a temperature-entropy (T-S) diagram as shown in Fig. 1. Here P_1, P_2, P_3 and P_4 are curves of constant external parameter. If we vary the parameter from P_1 to P_3 at temperature T_i, the entropy of the system will decrease from S_i to S_f. Now, if the parameter is varied back to P_1 adiabatically, the entropy of the system remains unchanged at S_f but the temperature will be decreased from T_i to T_f. In this way, the temperature of a working substance can be decreased if a suitable corresponding external parameter is found. The rapid drop of the higher curves P_1 and P_2 is due to the fact that the entropy is zero at absolute zero according to Nernest's Law.

2.2b PARAMAGNETIC SALTS

The use of paramagnetic salts as the working substance for temperature reduction was proposed independently by Debye (2) and Giauque (3) in 1926. They pointed out that some dilute paramagnetic salts can be used as the working substance because the magnetic ions in the lattice are relatively far apart, so

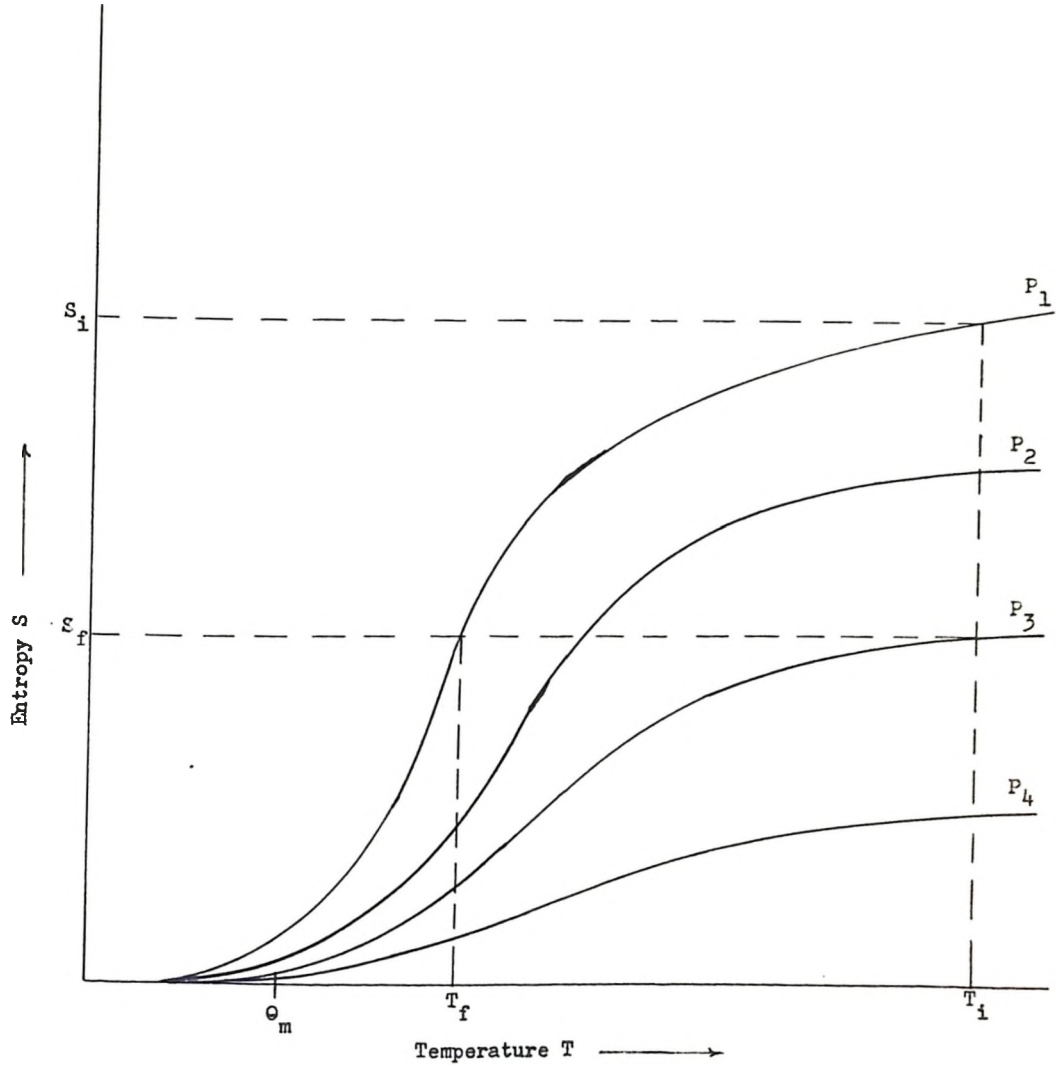

Figure 1. Entropy vs. Temperature

that their interaction energies are very small compared to the thermal energy at about $1^{o}K$. Hence, the spatial orientation is still randomly distributed and the entropy is considerable. If an external magnetic field is used as the parameter and if the potential energy of the magnetic ions in the field is comparable to the thermal energy at that temperature, most of the spins of these ions are oriented parallel to the applied field. Thus the magnetic entropy of the salt is lowered noticeably. We therefore, see that if a paramagnetic salt is magnetized isothermally and demagnetized adiabatically, the total entropy of the salt is decreased and the temperature of the salt should be expected to fall, because some of the lattice entropy is being shifted to the magnetic part.

Let us now consider a specific salt such as pink ruby in which the paramagnetic ions are Cr^{3+}. The free chromium ions is in a ^{4}F state, but due to the complete quenching of the orbital levels (11) at He temperatures, the effective state would then be ^{4}S. This four-fold ground level is split by the crystalline Stark splitting into two Kramers doublets (12), a distance δ apart, where $\delta = 0.3824\ cm^{-1}$ (13). These two spin doublets have levels of spin magnetic quantum number $\pm 3/2$ and $\pm 1/2$ along the trigonal axis. These magnetic moments have been verified by experiment (14). In applying a magnetic field of few thousand gauss these doublets are split into singlets by Zeeman splitting and the energy between the lowest and the highest level is at least that of the thermal energy kT, at helium temperatures.

According to Davis (15), the zero field susceptibility per unit volume of single-crystal synthetic ruby is given

$$\chi_o = \frac{N\mu_B^2}{kT}\left[\frac{9\exp\frac{a}{kT}+1}{\exp\frac{a}{kT}+1}\right]. \qquad (2.20)$$

N here is the number of Cr^{3+} ions per unit volume and a is the energy separation of the Kramers doublets. This expression may be expanded to obtain

$$\chi_o = \frac{C}{T-\Delta}, \qquad (2.21)$$

which is the Curie-Weiss Law. For an applied magnetic field parallel to the C-axis of the ruby crystal, $\Delta = 0.214^{\circ}K$ (16). In obtaining (2.20), Davis assumed that the $\pm$ 3/2 level lies lowest in Cr^{3+} and that the concentration of Cr^{3+} ions is small.

In view of (2.21), in the liquid helium temperature region, the susceptibility of ruby follows the Curie Law with very little deviation but at temperatures comparable to Δ, the Curie-Weiss Law must be used.

2.2c FINAL-TEMPERATURE DEPENDENCE ON INITIAL TEMPERATURE AND APPLIED MAGNETIC FIELD

From equation (2.21), it is clear that the lowest temperature that can be obtained by this method is $0.214^{\circ}K$. Below this, the substance becomes a ferromagnet. This, of course, is not the only factor which governs the final temperature for a given initial temperature and magnetic field. If we observe the T-S diagram

(Fig. 1) closely, for temperatures well below Θ_m, the entropy depends very little on the external parameter and thus the working substance loses its effectiveness as a good coolant below this point. Hence, this characteristic temperature Θ_m governs the final temperature as well.

In the above section we required a salt whose energy level separation should be small compared to the thermal energy when there is no field applied. Otherwise the salt is not very effective as a coolant for very low temperatures. In our case, the separation of the Kramers doublets in ruby is about one-third of the thermal energy during magnetization. Even though this does not meet the above requirement very well, there exist some properties (see Chapter IV) of ruby which are desirable in our experiment.

If the ruby is placed in a magnetic field H, the Kramers doublets are split into four singlets which are approximately $\mu_B gH$ apart. Due to the small field used in our case (4000 gauss), the separation between the highest and the lowest levels is $3\mu_B gH \sim kT_i$, where T_i is the temperature ($T_i \sim 1.5^\circ K$) during magnetization. Thus the distribution function can be expressed by the Boltzmann distribution and hence the entropy is determined by the ratio of $\frac{3\mu_B gH}{kT_i}$. If, after demagnetization the final temperature T_f obtained is of the order of Θ_m, the entropy is determined by the ratio $\frac{k\Theta_m}{kT_f}$. As the entropy remains constant during adiabatic demagnetization, we have

$$\frac{3\mu_B g H}{kT_i} = \frac{k\Theta_m}{kT_f}. \tag{2.22}$$

Therefore, $$T_f = \frac{k\Theta_m T_i}{3\mu_B g H}. \tag{2.23}$$

If the field is applied along the c-axis, g is approximately 2 for the Cr^{3+} ions in ruby. By substituting the numerical constants k, μ_B and g into equation (2.23) it reduces to

$$T_f = 2.15 \frac{\Theta_m}{H} T_i, \tag{2.24}$$

where H is in kilo-oersteds.

From the paramagnetic resonance data on ruby by Manenkov and Prokhorov (13), the separation of the Kramers doublets is $\delta = .3824\ cm^{-1}$. It is then reasonable to assume that when the thermal energy is equal to the separation of the doublets, the ruby loses its effectiveness as a coolant. Thus we can set $k\Theta_m$ equal to the separation. If this value of Θ_m is then substituted into equation (2.24) we obtain

$$T_f = 1.38 \frac{T_i}{H}. \tag{2.25}$$

From this, we may predict the final temperature of the ruby for an adiabatic demagnetization process.

2.3 THERMOMETRY

In order to construct a thermometer it is necessary to start with some reference points. There are quite a few such standard fixed-point which are used. At atmospheric pressure, points used are: 1336°K, the freezing point of gold; 373°K, the boiling point of water; 273°K, the freezing point of water; 4.22°K, the boiling point of liquid helium; 2.19°K, the lambda pt. of helium, and many other intermediate points. With these reference points, it is possible to construct and calibrate a thermometer.

There are many types of thermometers. The ones which are most commonly used are: gaseous and resistance thermometers, thermocouples and vapour pressure of some gases. Thermocouples are often used in the high temperature region, Gas thermometers in the intermediate region and resistance and vapour pressures are used in the intermediate and low temperature region. At very low temperatures, the vapour pressure of helium is so small that it is useless as a thermometer. Consequently other means must be applied.

After the development of the Curie Law, it was found that many paramagnetic salts follow this law to very low temperatures. Hence, by making use of the Curie Law $\chi = \frac{C}{T}$, it is possible to calibrate the susceptibility of a paramagnetic salt at temperatures between 1-4.2°K and then use it as a thermometer below 1°K by extrapolating the calibration curve to lower temperatures. Subsequently, the corresponding temperature may be

deduced if the susceptibility below $1^{\circ}K$ is known. Since no paramagnetic substance follows the Curie Law perfectly down to absolute zero, a correction must be made to the Curie-Weiss Law at very low temperatures.

CHAPTER III

APPARATUS

3.1 ADIABATIC DEMAGNETIZATION CRYOSTAT

The final demagnetization cryostat design is as shown in Fig. 2. With reference to this figure and starting the description from the inside, we have a high-vacuum chamber in which the ruby crystal is situated. Fitted tightly outside the chamber is a pair of mutual inductance measurement coils wound on a plexiglas coil form (see Fig. 5). Immediately outside these coils is the superconducting magnet (solenoid) which is also wound on a plexiglas coil form (see Fig. 5). This inner system, which will be described in more detail later in this chapter, is surrounded by a conventional strip-silvered liquid helium dewar and liquid nitrogen dewar, both of the standard glass type. The liquid helium dewar is connected through a 6-inch pumping line to a rotary pump (Edwards High Vacuum, Model ISC3000) with a rated pumping speed of 2,830 litres per minute. With this pump, it was possible to reduce the temperature of the helium bath to about $1.4^{\circ}K$ by reducing the vapour pressure of the liquid helium. The helium bath temperature would be controlled over the range $1.4 - 4.2^{\circ}K$ with the aid of a 1-inch Vecco valve in series with the pumping line. A carbon resistance heater was also included in the

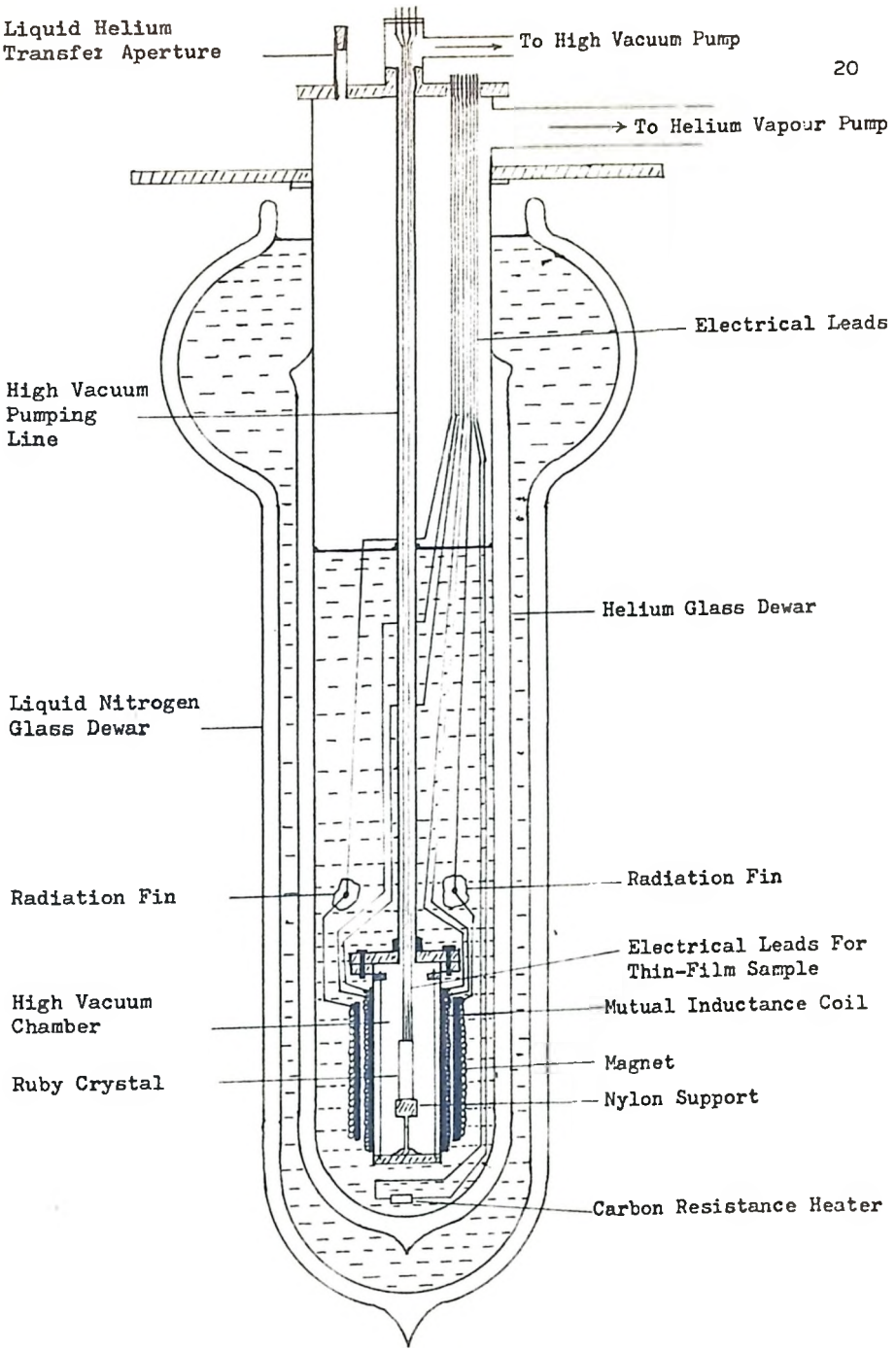

Figure 2. Demagnetization Cryostat

helium bath for further temperature control.

3.2 TEMPERATURE MEASUREMENT DEVICES

In these experiments, two temperature measurement devices were used. Over the normal range of helium bath temperatures, vapour pressure thermometry was employed with the aid of a standard mercury manometer (see Fig. 3 and 8) and Bureau of Standards pressure-temperature conversion tables (17). These temperatures as well as temperature levels below 1°K could also be monitored with the aid of a paramagnetic susceptibility thermometer.

In a paramagnetic susceptibility thermometer of the type described below, temperature changes in a paramagnetic specimen may be related to the mutual inductance changes when this specimen is coupled to a mutual inductance system. The relationship between mutual inductance and susceptibility - a linear one - has been adequately described by de Klerk (18) and Lawrence (19) and the derivation will subsequently be omitted here. Mutual inductance measurements may be made on such a paramagnetic specimen over a known region of temperature and such temperature characteristics can be extrapolated to lower regions if the susceptibility characteristics of the specimen are known.

In these experiments, an a-c mutual inductance bridge (Cryogenics, Inc. Ml. 155B) of the Hartshorn type was employed as shown schematically in Fig. 4. In this diagram, C_2 is a continuous variable built-in inductance, R is the resistance in the circuit, S is the specimen under investigation, SG is the

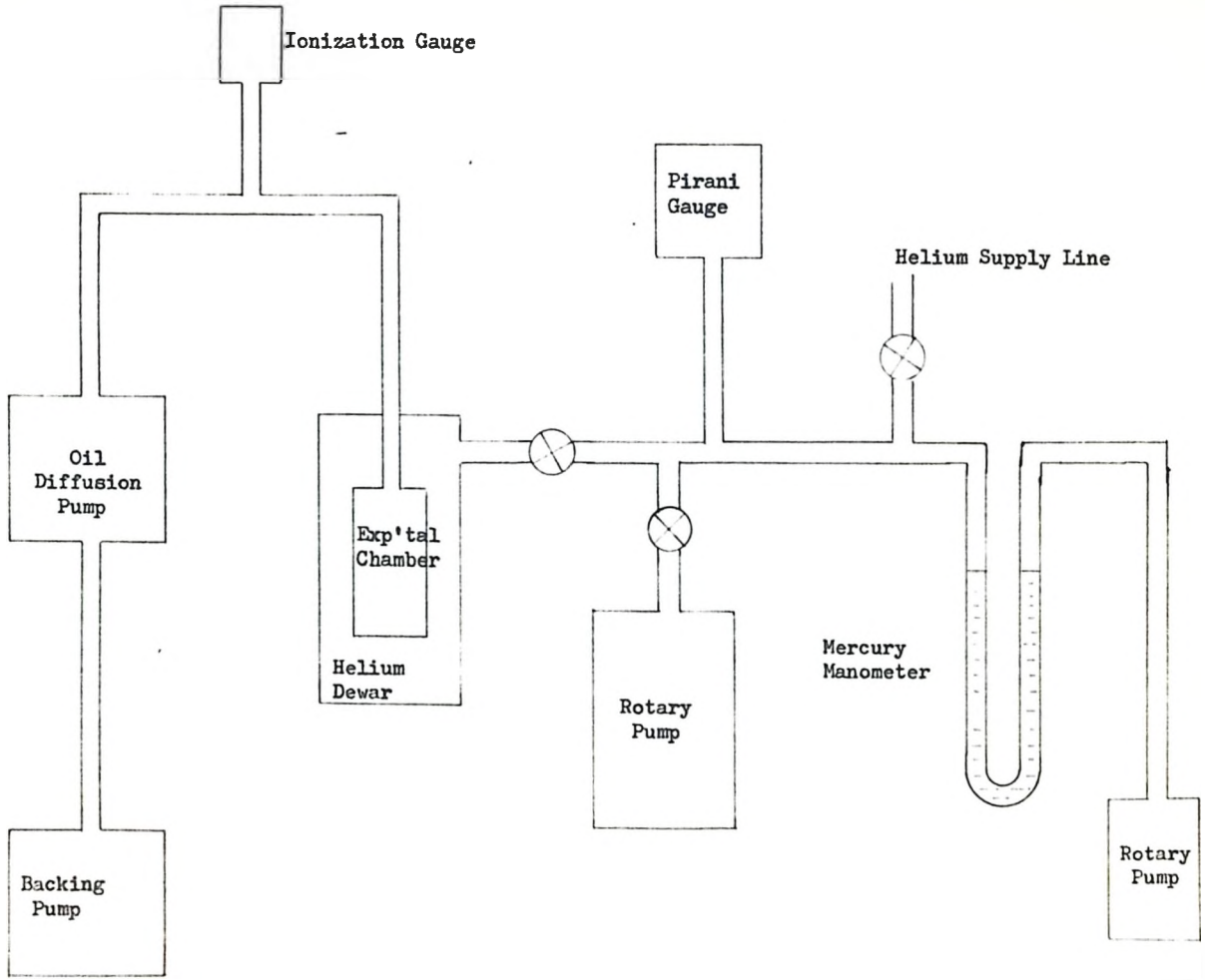

Figure 3. Vacuum System

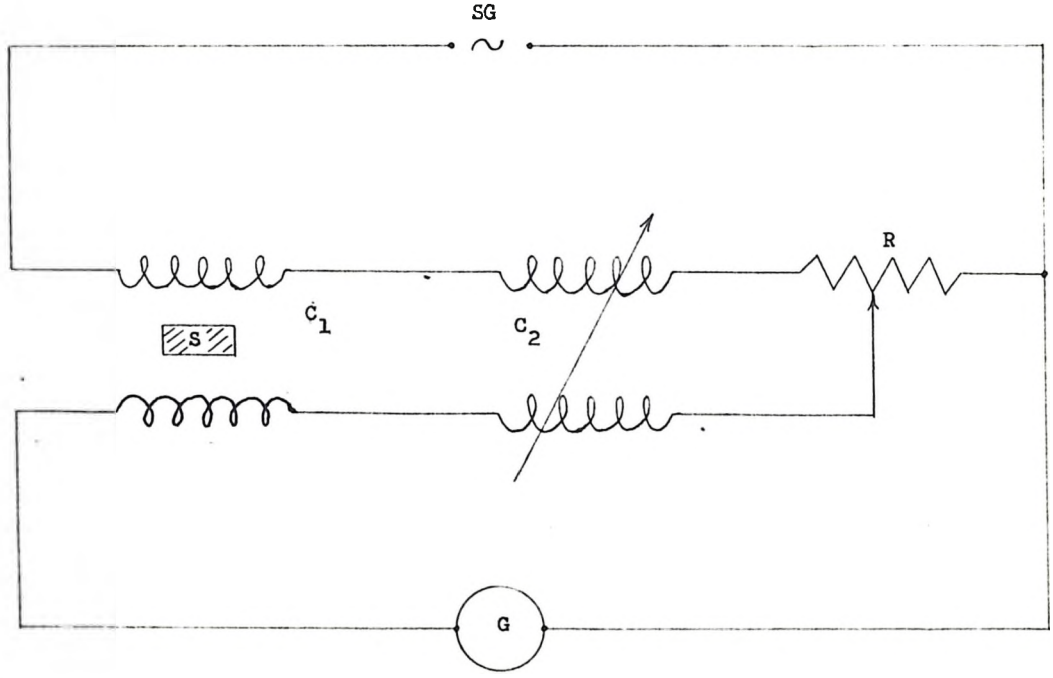

Figure 4. Alternating Current Hartshorn Bridge

audio frequency generator and C_1 is the pair of mutual inductance coils used in measuring the change in susceptibility of the specimen. An oscilloscope G (Solertron CD1014.2) is used as the bridge null detector. By balancing the bridge at different temperatures, the relative change in mutual inductance and consequently susceptibility may be obtained. The bridge has a resolution of better than 8×10^{-4} µh in the range 0 to 200µh. A more detailed description of the electronics and operation of this bridge has been given by Lawrence (19).

Coil C_1 consists of two concentrically wound coils - a primary and a secondary - on a 4 1/4" long plexiglas coil form which fits tightly outside the high-vacuum chamber. The secondary is divided into three parts. The sections at the two ends are wound in opposition to the mid-section. The total length and number of turns of the ends are approximately equal to that of the mid-section. This is desirable because it eliminates the net mutual inductance between the coils in the absence of the salt and thus maximizes the observable changes when the salt is included. The primary consists of 1390 turns of #36 copper wire and the secondary has 560 turns in the mid-section and 257 turns at each end. In order to eliminate the drift of the bridge due to the variation of resistance of the leads down the cryostat with temperature during the experiment, leads of constant resistance (#36 Karma wire) are used. Also, resistors were placed in series with the primary and secondary coils to mack out any further change in resistance.

3.3 SUPERCONDUCTING MAGNET

Superconducting silk-insulated cold-worked niobium wire was used in the construction of the superconducting magnet (solenoid). 3300 turns of #36 niobium wire were wound on a plexiglas coil form of 1 1/4" in diameter and 3 1/4" in length which can be fitted just outside the mutual inductance coils. It was necessary to keep not only the solenoid below the helium-bath level but also the niobium leads proceeding from the solenoid to the power supply. This latter step eliminated the excessive joule-heat generation that would otherwise occur in the normal-state niobium with the flow of large supply currents. The niobium leads were therefore connected below the helium-bath level to copper input leads, which in turn were connected to external 40 volt-25 amp regulated power supply (Type-Harrison Laboratory Inc., Model 520A), through Kovar feed-through leads on top of the cryostat.

Detrimental joule-heat generation could still be produced, however, by high contact resistance between the copper and niobium wires. In this respect, it has been shown (20) that joule-heat generation at such contacts can initiate travelling temperature wave along the niobium which, if not sufficiently dissipated by the helium bath, can destroy the superconductivity of the solenoid at current values much lower than anticipated by Silsbee limit. In order to obtain the highest critical current through the solenoid, this contact resistance was minimized by the method employed by Autler (21). That is, the niobium wires from the solenoid were spot-welded to two short 0.020" platinum wires following which the

platinum wires were soft-soldered to the copper leads coming down from the top of the cryostat. These leads consist of twin #30 copper wires from the Kovar lead-through connector to a point about halfway down the dewar with single #30 copper wires proceeding from this point to the platinum wires. Besides the spot-welding to reduce the contact resistance, thin copper fins were attached to the junction of niobium and platinum wires to dissipate any joule-heat generation remaining at the joint. With this arrangement, a maximum "quenching" current of 10-11 amps would be obtained, with a resulting maximum field of 4000 gauss in the solenoid. Such fields could be monitored with the aid of a Hall-Effect fluxmeter (Type-Bell "240" Incremental Gaussmeter) and external longitudinal probe.

3.4 EXPERIMENTAL LOW-TEMPERATURE, HIGH-VACUUM CHAMBER

In constructing this chamber, careful consideration was given to the choice of the material because it must be a good thermal conductor and a non-ferromagnetic material at low temperatures. A good thermal conductor is required as it must be able to conduct the heat of magnetization to the helium bath quickly while the salt is being magnetized. A non-ferromagnetic material is necessary otherwise the mutual inductance measurements would be offset. With these problems in mind, a thin-walled (0.010") seamless stainless steel tubing of 1" O.D., 4 1/2" in length with similar material for top and bottom flanges, has been used (see Fig. 5). These flanges were silver-soldered on so that no ferromagnetic properties were introduced in the soldering process. The flange at the bottom

Magnet | Ruby Crystal and Holder | Chamber | Aluminum Gasket | Mutual Inductance Coil

Figure 5.

of the chamber has the same diameter as the chamber itself so that the plexiglas inductance coil form may slide on it tightly. The flange at the top is 1 3/4" in diameter with six evenly distributed threaded holes (see Fig. 5). At the open end of the chamber a matching flange was bolted to the top flange of the chamber by six screws with an indium O-ring as a vacuum seal. Through this removable flange, three thin-walled (0.012") stainless steel tubings, size 1/4", 1/8", 1/16" O.D., were soldered. The upper ends of these tubings were led through, and also soldered to, the cryostat top plate (see Fig. 6a). The 1/4" tubing was used as the pumping line for the chamber; the 1/8" tube, sealed at the top with a Kovar lead-through, provided a means for electrical leads (#40 copper wires) to enter the chamber. Finally, the 1/16" tube was connected to an ionization pressure gauge.

The pumps used for the vacuum chamber consisted of a 2 1/2" oil diffusion pump (Type-Edwards High Vacuum, Model E02) and a backing pump (Type-Welch, Model 1400) with a pumping speed of 21 litres/second.

The design of the matching flange mentioned above had two disadvantages and consequently it was replaced by a new one. The disadvantages were that induced persistent current's magnetic fluxes in the superconducting indium ring caused erroneous mutual inductance readings. Further, the pumping line to the ionization gauge was too constricted and seriously reduced the effective pumping speed at the sample chamber.

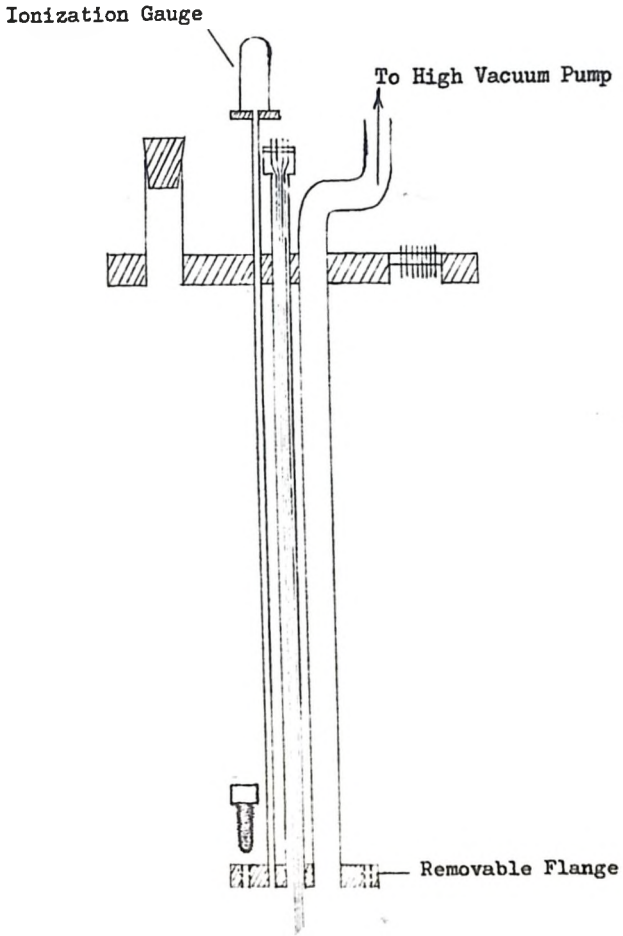

Figure 6a. Top Plate and Removable Flange

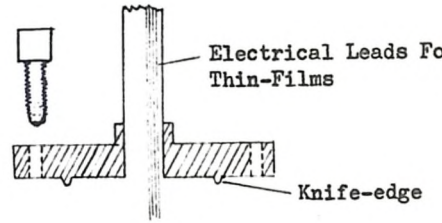

Figure 6b. Final Design of Removable Flange

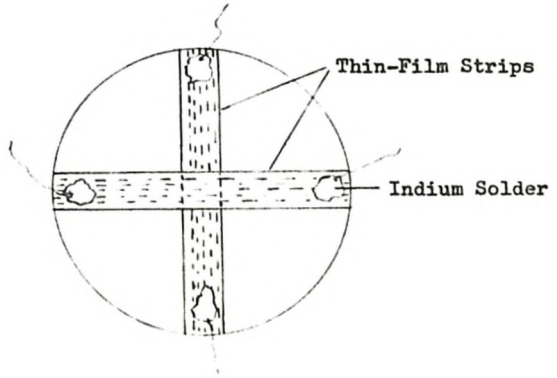

Figure 6c. End of Ruby Crystal with Thin-Films

In order to overcome these difficulties, only a single 1/4" O.D. stainless steel tubing was finally used (see Fig. 7), both as the high vacuum pumping line and the means of electrical lead inlet. The electrical leads, intended for thin-film experiments, were taken through the Kovar lead-through (see Fig. 7) to the external equipment of the type discussed by Dynes (22). To seal the chamber, a knife-edge on the new removable flange was used to contain an aluminum gasket (see Fig. 6b and 5). On top of the plate which seals the helium dewar, the high vacuum pumping line is increased from 1/4" to 1/2". The bellows shown on the pumping line (see Fig. 8) provide an easy means of removing the inner chamber system with the glass dewars in situ. The pressure of the inner chamber system is measured by the ionization gauge and read on a meter (Type-Edwards High Vacuum Ionization and Pirani Vacuum Gauge, Model 1) (see Fig. 8). The needle valve just above the bellows is used as the helium exchange gas inlet during magnetization.

3.5 RUBY CRYSTAL AND ITS SUPPORT

The ruby crystal (see Fig. 5) used is pink and has a cylindrical shape with dimensions 2 inch x 1/4 inch diameter. It weighs approximately 5 grams and the magnetic ion (Cr_2O_3) concentration is about 0.05% by weight. Ruby was chosen as paramagnetic salt for this experiment because it possesses three important and desirable properties as a coolant below 1°K (16):

(1) chemical and physical stability.

(2) good thermal conductor.

(3) adequate thermal contact between it and any metallic

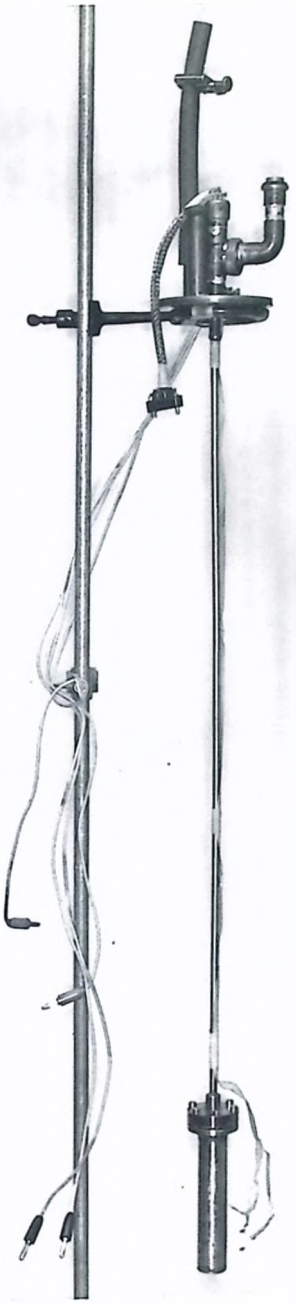

Figure 7. Helium Dewar Top-Plate and Chamber Attachment

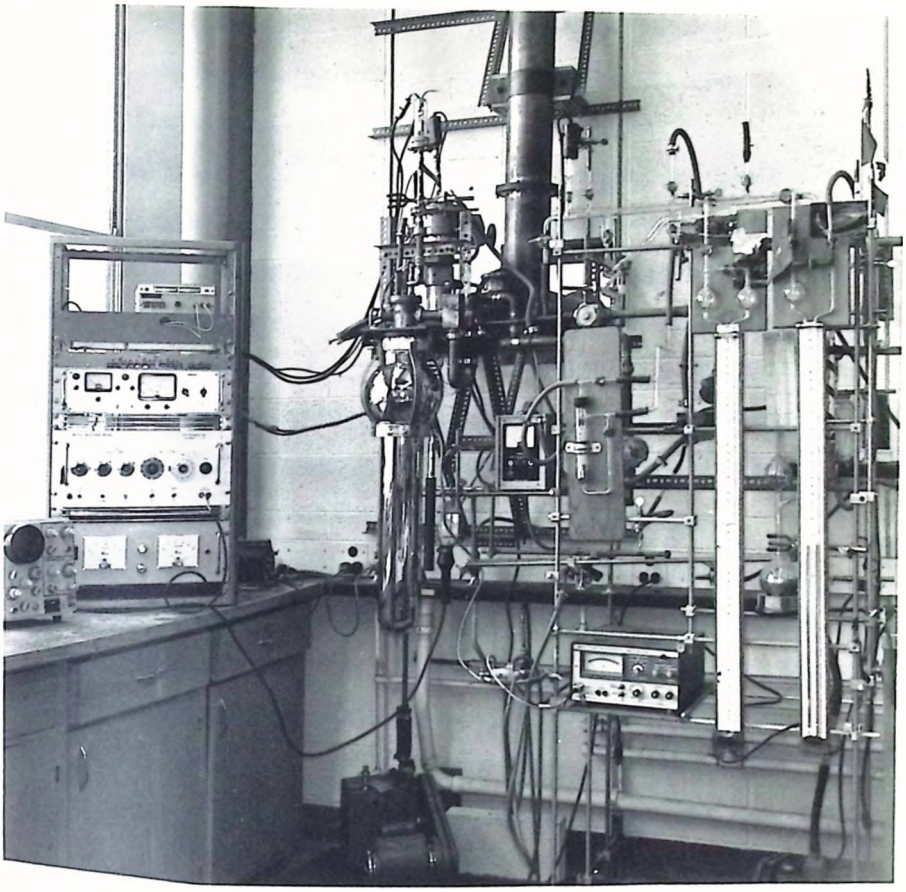

Figure 8. Complete Experimental Apparatus

thermal links.

To support the crystal in the centre of the chamber, a squirrel cage centering device is used (see Fig. 5). The cup holding the crystal, the stem and the centering rings are made of nylon. This material was chosen because it is a very poor thermal conductor and good thermal insulation is needed during and following demagnetization process. This thin stem was used to minimize possible heat leaks. The three non-ferromagnetic stainless steel rods along the generator of the cage are used to give rigidity to the holder. The holder was made such that it can slide into the chamber easily and yet have little or no movement laterally. This rigid support is desirable since vibrations of the crystal can increase the amount of heat influx.

3.6 SUPERCONDUCTING THIN-FILMS

Besides magnetizing the ruby crystal with different fields it was also our aim to attempt to evaporate thin superconductive tunnel junctions at the end of the crystal and examine them at low temperatures using the ruby as the cooling agent. To deposite the films, the ends were first cleaned with Ajax cleanser and following the standard deposition procedures (23), an Al-Al_2O_3-Pb superconducting barrier junction was deposited on one end of the crystal as shown in Fig. 6c. The electrical circuit to the thin-films was completed with the aid of #40 copper wires proceeding down the cryostat and attached to the films with indium solder.

CHAPTER IV

RESULTS

4.1 PERFORMANCE OF MAGNET AND MUTUAL INDUCTANCE COILS

4.1a MAGNET

The first method used to make the contact between the copper leads and the niobium wires onto thin copper radiation fins was by means of screws and nuts, soft-soldering the ends of the copper wires directly onto the fins. Due to the poor contact between the niobium wire and the fin, a maximum d-c current of only 5 amps could be applied before the wire at the junction became normal and burned off. This problem was overcome by spot-welding as mentioned in Chapter III. The maximum d-c quenching current which can be applied with this arrangement is above 10 amps. This arrangement also desirably reduced the helium boil-off rate during magnet operation.

4.1b MUTUAL INDUCTANCE MEASUREMENTS

The final mutual inductance measuring circuit appeared to be quite stable and accurate under operating conditions. To ensure this result it was necessary to keep to a minimum any relative changes in the resistance of the bridge circuit that would result from the falling liquid helium level within the cryostat. In this particular bridge circuit any such large changes - if permitted to occur - could introduce a false change in the apparent mutual inductance reading, even when the temperature

of the paramagnetic salt was kept constant at 4.2°K. This possible source of error was eliminated in the final design by the use of "Evenohm" (#36 Karma wire) constant resistance input leads to the mutual inductance coils, in series with 3000 ohm stable resistances located in the external circuit. With this final design the spurious change of apparent mutual with liquid helium level was found to be negligible. Drift effects attributed to the external circuitry was estimated to be within 1%.

It should be noted that all mutual inductance measurements were made with the magnet input leads disconnected. This was done to avoid any spurious coupling between the mutual inductance circuit and the magnet circuit that would affect the apparent mutual inductance reading.

4.2 DEMAGNETIZATION MEASUREMENTS

A full description of the steps and precautions required during adiabatic demagnetization does not appear to exist in the literature, let us consider these in detail as applied to our experiments. We have a paramagnetic salt located in a vacuum chamber which itself is immersed in liquid helium. By letting helium exchange gas into the chamber, the gas acts as a heat conducting medium which cools the salt to the temperature of the helium bath. When this condition has been attained, the magnet is switched on and the heat of magnetization generated in the salt is allowed to dissipate through the exchange gas to the helium bath. This corresponds to the isothermal process mentioned

in the previous chapter. The helium gas is then pumped out leaving the salt thermally isolated in the vacuum chamber. The magnet is then turned off. This is the adiabatic demagnetization step.

Before proceeding with a demagnetization experiment, however, a very useful and necessary preliminary experiment should be performed if metal vacuum chambers are employed. Mutual inductance experiments should be made down to the pumped helium low temperature range to determine whether or not undesirable ferromagnetic transitions occur in the chamber material over these temperatures. When this test was carried out by us it was found that in the absence of the salt the mutual inductance remained unchanged as shown in Fig. 9 and hence it was concluded that no undesirable ferromagnetic materials were present in the chamber.

It has been suggested by White (24) that during magnetization the helium exchange gas pressure should be approximately 10^{-3} mm. of Hg. If it is above 10^{-2} mm., the heat leak after demagnetization may be large and if below 10^{-4} mm. the heat of magnetization may not be removed efficiently. In this experiment, we found that, in this respect, exchange gas pressures between 7×10^{-4} and 10^{-3} mm. of Hg gave the best results. We found that 10 to 15 minutes operation with these exchange gas pressures was sufficient for the removal of the heat of magnetization. Following this step, at least 8 minutes were required to evacuate the chamber to a pressure of $\sim 2\times10^{-5}$ mm. of Hg. At this pressure, thermal inculation appeared to be adequate, for after demagnetization the final temperature as monitored by the mutual inductance bridge remained

Figure 9. Susceptibility vs. Inverse Temperature

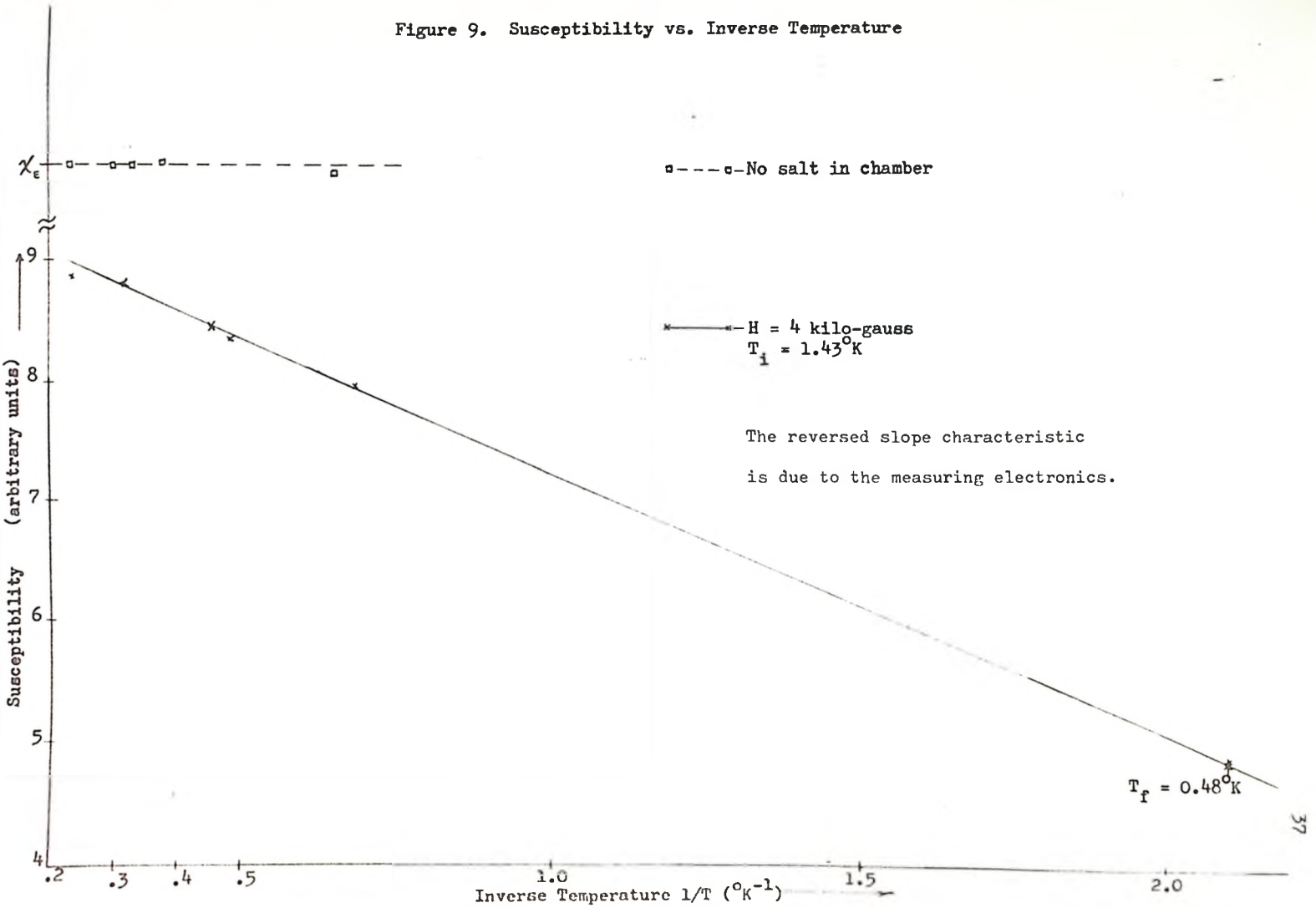

unchanged for at least 5 minutes. This also means that the heat leak through the thin nylon stem supporting the ruby and down the stainless steel pumping tube was reasonably small.

A typical experimental curve which indicates the calibration and the final temperature obtained after demagnetization is shown in Fig. 9. The points in the temperature range of 1.5-4.2°K (i.e., 0.238-0.667°K^{-1} on the 1/T scale) are used in the calibration. It can be seen clearly that in this region, the experimental susceptibility obeys the Curie Law quite well. Fig. 9 also shows that the final temperature reached by using a field of 4 kilo-gauss is 0.48°K. This final temperature in this instance was calculated by extrapolation based on a Curie-Law susceptibility relationship. (This, of course, is not the true absolute temperature and a correction must be made as will be indicated in the following section). The susceptibility reading at this point was measured within 1 minute after the magnet was switched off. This time delay was sufficiently long to assure thermal equilibrium since the spin-lattice relaxation time of ruby is small ($\sim 10^{-2}$ sec.) (25) and since at this temperature ruby is a very good thermal conductor.

4.2a TEMPERATURE CORRECTION USING DAVIS' RELATION

Davis' relation for susceptibility and temperature was given in Chapter II by equation (2.20). This equation reduces to the same form as the Curie-Weiss Law which means that at low temperatures the susceptibility-temperature relation deviates from the Curie Law. Consequently, a correction must be made to the final temperatures obtained above as calculated from the Curie relationship. By normalizing the equations (2.20) and (2.7) at 4.2°K, both the Davis and Curie

characteristics may be plotted as shown in Fig. 10. From these curves, the final true absolute temperatures reached in the experiments can be determined by picking the corresponding temperature on the Davis Curve when a certain is given on the Curie Curve. (i.e., $0.48^{\circ}K$ on Curie Curve corresponds to $0.52^{\circ}K$ on Davis Curve).

A plot of the final-temperature versus the magnetic field applied is shown in Fig. 11. On the same figure, the theoretical curve calculated from equation (2.25) is also plotted. From the form of (2.25),

$$T_f = 1.38 \frac{T_i}{H}, \qquad (2.25).$$

T_f would appear to go to infinity at H=0 and to zero for large H. This obviously can not be the case because if H=0 the final temperature should be $T_f=T_i$. Further, if H is large, saturation effects due to the ordering of the spins in the system and the constant lattice entropy which is not affected by the field would limit the lowest obtainable temperature. These asymptotic effects show up very clearly in Fig. 11 as the two curves intersect each other at low values of H and at high values of H, (4 kilo-gauss), the theoretical values remain below the experimental values. Discounting these asymptotic effects, the results agree, to within 10%, with the calculated values, even though these values were determined only for the case in which $kT_i \sim 3\mu gH$. Hence, within the field range where the theory is applicable, the final temperature of the ruby crystal

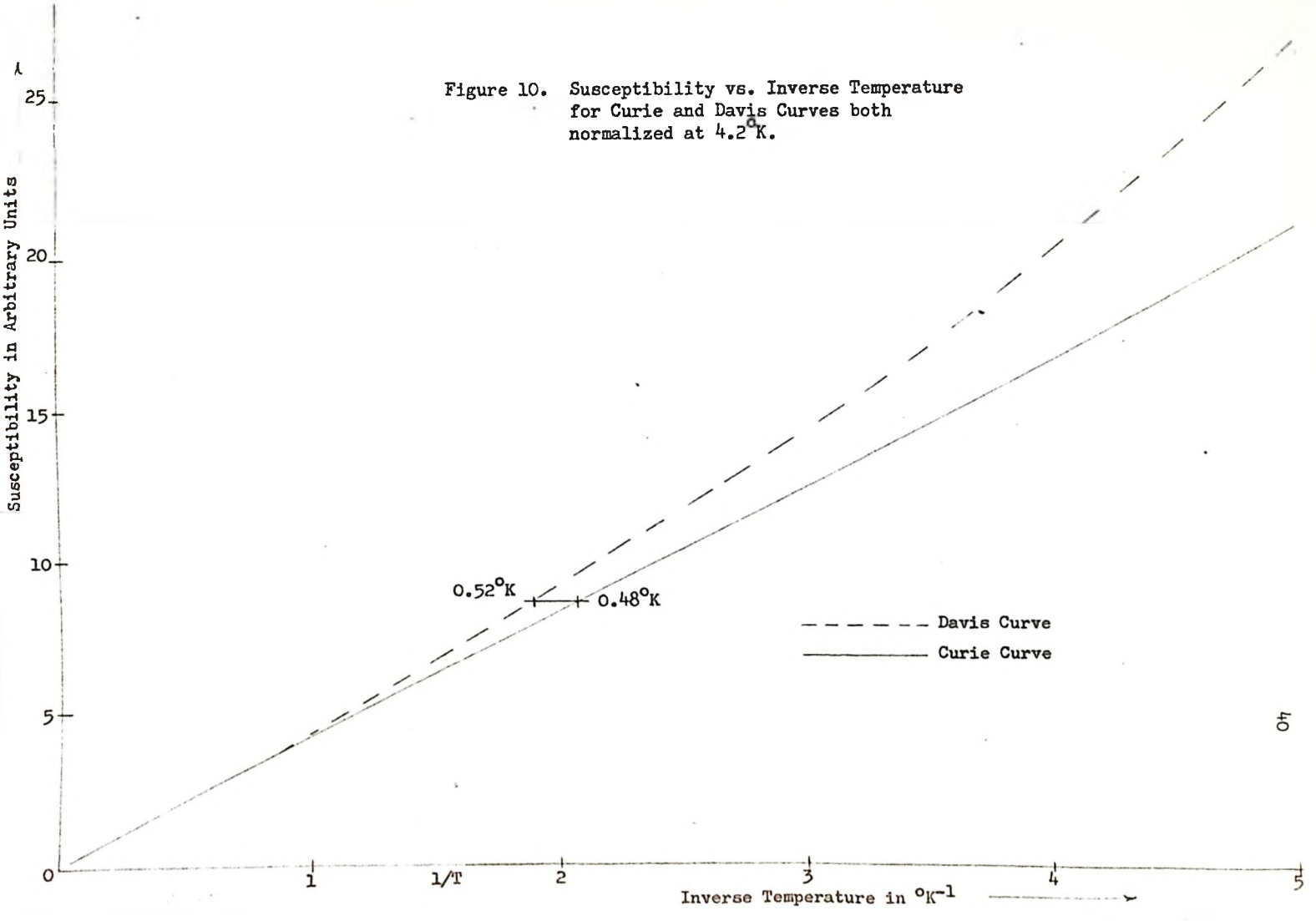

Figure 10. Susceptibility vs. Inverse Temperature for Curie and Davis Curves both normalized at 4.2°K.

Figure 11. Final-Temperature vs. Applied Magnetic Field

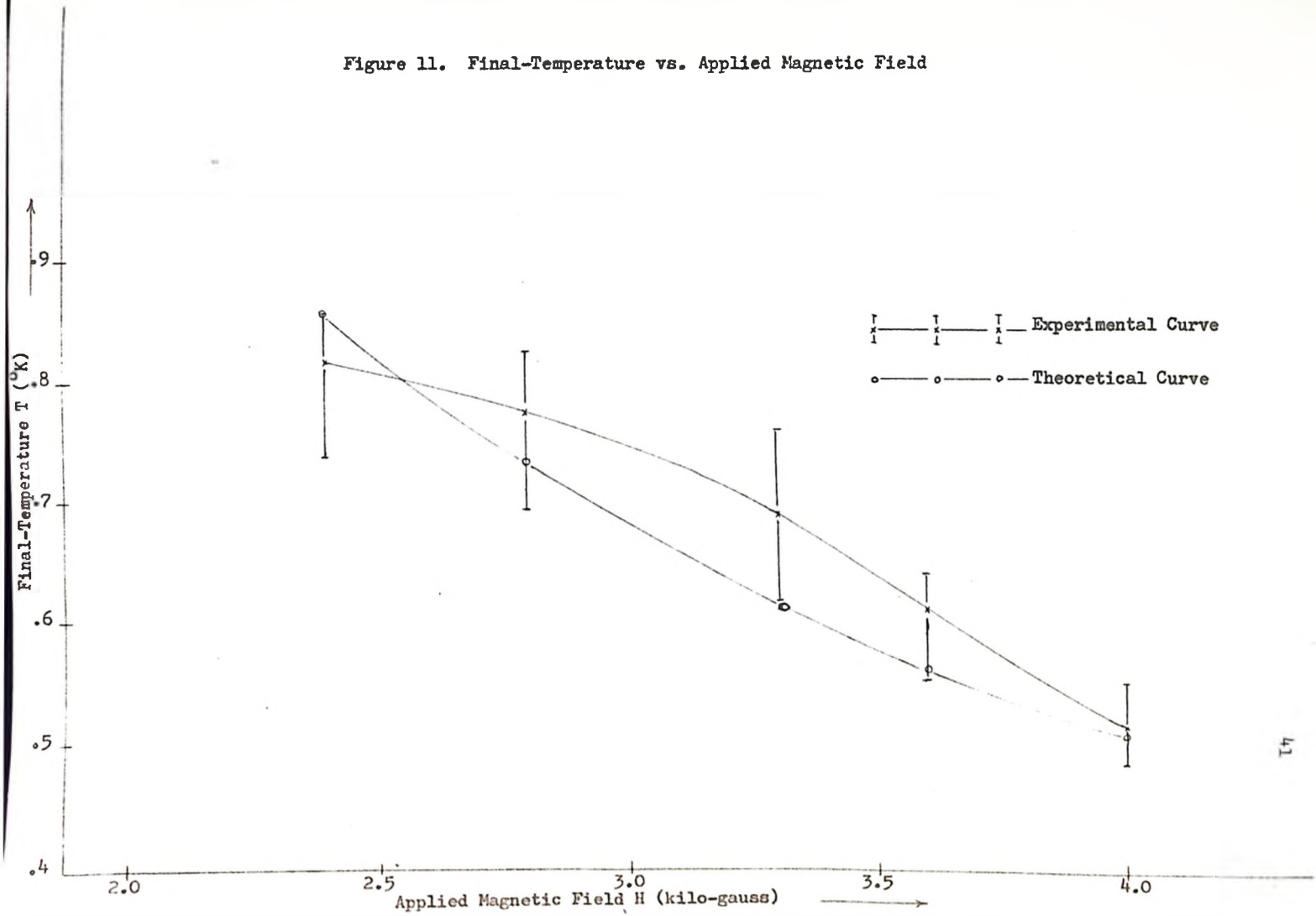

may be predicted with reasonable success when the initial temperature is known.

4.3 SUPERCONDUCTING THIN-FILMS

In preliminary experiments on superconductive tunneling, an Al-Al_2O_3-Al barrier junction was evaporated onto an end of the ruby crystal. Such a junction showed no expected non-linear superconducting current-voltage, I-V, tunneling characteristics even after demagnetization in the field of 4 kilo-gauss. This particular experiment did not give anything conclusive because the susceptibility measurements indicated that there was a decrease in temperature. In order to find what was happening, we replaced the Al-Al_2O_3-Al sample with an Al-Al_2O_3-Pb sample. The advantage in using this is that lead goes superconducting at 7.2°K and hence non-linearI-V characteristics should be observed before magnetization. With this sample, non-linear I-V characteristics were indeed observed before magnetization but not after. Also, these characteristics were indicated only when the helium exchange gas was present in the chamber. Two possible explanations may be given for this effect:

(i) the heat-leak down the #40 copper wires to the films was so large that when the chamber is evacuated the heat goes directly to the film and the salt only. Consequently, the salt and the films remain at relatively high temperatures.

(ii) With even small heat leaks, the surface layer of the ruby (26) may be at a much higher temperature than the inside of the crystal.

Further attempts were made on this by taping the #40 copper

wires onto the top flange of the chamber using masking tap. This arrangement was intended to give thermal anchoring at 1.4°K, but since thermal contact between the wires and flange was rather poor, results similar to above were obtained.

CHAPTER V

CONCLUSIONS AND RECOMMENDATIONS

The main aim of this experiment is to observe the variation of the final temperature obtained with different magnetic fields for a synthetic ruby crystal using the method of adiabatic demagnetization. Also it was our intention during the construction of the experimental chamber that this apparatus would be used in thin-film applications using the ruby as the cooling agent.

The results obtained for the temperature-field experiments seem to agree fairly well with the extremely simple theory developed here. A more rigorous theory may be developed in the same way. For instance, during magnetization in the field H, the low lying orbital singlet energy levels of ruby are given by Davis (15) and hence the total entropy of the system may be calculated from

$$S = -k \sum_{m=1}^{4} f_m \ln f_m, \qquad (5.1)$$

where f_m is the probability function or the Fermi-Dirac distribution function for the level m. The entropy after demagnetization may also be obtained in a similar manner except now there are only two degenerate levels instead of four non-degenerate levels. By equating the entropy during and after magnetization we may find

the dependence of the final-temperature on the magnetic field and the initial temperature.

If this system is to be used as a coolant for thin-film work, a few improvements should be made:

(i) Elimination of the heat leak through the electrical leads.

This may be achieved by using a better method for the thermal anchoring of the copper wires. If these leads were taken out of the chamber and wrapped and cemented or glued about 2 feet in length around a copper post immersed in liquid helium, the amount of heat leak would be drastically reduced. Also poor thermal conductors such as german-silver, which has a conductance about 1000 times less than that of copper at helium temperatures, should be used as leads.

(ii) Paramagnetic salt.

A higher concentration of Cr^{3+} ions (0.5%) is desirable because with the field now available lower temperatures may be obtained. If this final temperature is near the Curie point, it will remain there for a much longer period because of the high specific heat near the Curie point. Also a crystal of larger diameter is preferred especially in the thin-film experiments.

Other salts whose Curie points are much lower may be used for even lower temperatures. Ferric alum is one of these salts. If it is compressed into a pill of cylindrical shape, it could be used as a coolant for thin-film work. Of course, in order to obtain temperature homogeneity in Ferric alum, the pill should

contain fine bare copper wire mesh to give good thermal conduction throughout it and in order to cool the substrate of the film these copper wires should all be attached to a thin copper disc at one end of the cylinder. A sapphire substrate, an excellent thermal conductor, would then be cemented onto the disc for thin-film deposition.

(iii) Higher field magnet.

A higher field superconducting magnet would give lower final temperatures than those obtained in this experiment.

(iv) Apparatus.

The continuous flow of helium exchange gas into the chamber during magnetization should be eliminated because this continuous flow may introduce undesirable external heat into the chamber. Thus an extra vacuum tight valve is needed just on top of the cryostat to seal off the chamber after the helium exchange gas is admitted into the chamber.

BIBLIOGRAPHY

1. Zemansky, A. C., Heat and Thermodynamics, p. 397.
2. Debye, P., Ann. Phys. 81, 1154, (1926).
3. Giauque, W. F., J. Amer. Chem. Soc. 49, 1864-1870, (1927).
4. Giauque, W. F., McDougall, D. P., Phys. Rev. 43, 768, (1933).
5. de Haas, W. J., Wiersma, E. C., Kramers, H. A., Nature 131, 719, (1933).
6. Kurti, N., Simon, F., Nature, Lond. 133, 907, (1934).
7. Mendelssohn, K., Moore, J. R., Nature, Lond. 133, 413, (1934).
8. Daunt, D. G., Mendelssohn, K., Nature, Lond. 143, 719 (1939).
9. Kurti, Robinson, Simon, Spohr, Nature 178, 450, (1956).
10. Daunt, J. G., Edwards, D. O., Kreitman, M., Pandorf, R. C., Snider, J. W., Proc. of VIIth Int. Conf. on Low Temperature Physics, p. 96, (1960).
11. de Klerk, D., Handbuch der Phys., Low Temperature Physics II 15, 44, (1956).
12. Kramers, H. A., Proc. Acad. Sci. Amst. 33, 959, (1930).
13. Menenkov, A. A., Prokhorov, A. M., J.E.T.P., Physik USSR 28, 762, (1955).
14. Henry, W. E., Phys. Rev. 88, 559, (1952).
15. Davis, H. L., Z. Phys. Chem. Neue Folge 16, 213-217, (1958).
16. Daunt, J. G., Brugger, K., Z. Phys. Chem. Neue Folge 16, 203-212, (1958).

17. The "1958 He^4 Scale of Temperatures", U.S. Dept. of Comm., N.B.S.

18. de Klerk, D., Handbuch der Phys., Low Temperature Physics II 15, 75, (1956).

19. Lawrence, H. J. O., M. Eng. Thesis, McMaster Univ., (1965).

20. Campbell, C. K., Walmsley, D. G., Can. J. of Phys. 41, 416, (1963).

21. Autler, S. H., Rev. Sci. Instr. 31, 369, (1960).

22. Dynes, R. C., M.Sc. Thesis, McMaster Univ., (1965).

23. Walmsley, D. G., Ph.D. Thesis, McMaster Univ., (1965).

24. White, G. K., Expt'al Tech. in Low Temperature Physics, p. 243, (1961).

25. de Klerk, D., Handbuch der Phys., Low Temperature Physics II 15, 166, (1956).

26. Mendoza, E., Proc. of VIIth Int. Conf. on Low Temperature Physics, p. 117, (1960).